Finite Element Modeling and Parametric Analysis of Pavement Dynamic Responses under Moving Vehicle Load

LIU Xiaolan[1], *ZHANG Xianmin*[2,3*]

1. Civil Engineering College, Tianjin Chengjian University, Tianjin 300384, P. R. China;
2. College of Civil Aviation, Nanjing University of Aeronautics and Astronautics, Nanjing 211106, P. R. China;
3. College of Airport Engineering, Civil Aviation University of China, Tianjin 300300, P. R. China

(Received 8 March 2019; revised 5 May 2019; accepted 25 May 2019)

Abstract: This paper intends to develop finite element models that can simulate vehicle load moving on pavement system and reflect the pavement response of vehicle and pavement interaction. We conduct parametric analysis considering the influences of asphalt concrete layer modulus and thickness, base layer modulus and thickness, and subgrade modulus on pavement surface displacement, frequency, and strain response. The analysis findings are fruitful. Both the displacement basin width and maximum value of dynamic surface displacements are larger than those of static surface displacements. The frequency is positively correlated with the pavement structure moduli, and negatively correlated with the pavement structure thicknesses. The shape of dynamic and static tensile strain is similar along the depth of the pavement structure. The maximum value of dynamic tensile strain is larger than that of static tensile strain. The frequency of entire pavement structure holds more significant influence than the surface displacement and strain do. The subgrade modulus has a significant effect on surface displacement, frequency and strain.

Key words: pavement dynamic response; vehicle load; surface displacement; frequency; strain

CLC number: U416 **Document code:** A **Article ID:** 1005-1120(2020)03-0490-11

0 Introduction

Finite element (FE) models play an important role in explaining the pavement response subjected to moving vehicle loading. Garcia et al.[1] explicated that transverse tensile strains were more responsible for fatigue cracking compared with longitudinal strain in terms of strain magnitude and pulse duration. Picoux et al.[2] predicted the asphalt pavement displacement response with the stationary transient load placing on the asphalt surface. Wang et al.[3] simulated vehicular loading as moving transient load to study the strain response of the asphalt pavement. Ozer et al.[4] researched the effect of bonding conditions on the critical strains in hot-mix asphalt (HMA) overlaid Portland cement concrete (PCC) pavements by laboratory experiment, field testing, and numerical analysis. They found HMA tensile strains can be significantly amplified with less stiff interface properties which correspond to decreasing bonding strength. Wang et al.[5] and Al-Qadi et al.[6] applied the viscoelastic model of asphalt pavement to investigate the effect of wheel load, vehicle speed, pavement structure, and temperature on modulus distribution in the granular base layer. Patil et al.[7] proposed a solution algorithm of three-dimensional finite element analysis to analyze the dynamic response, including displacement and velocity, of pavement structure with moving vehicle loading. The study by Dong and Ni[8] showed that vertical compression strain at the top of the asphalt layer was a key index to evaluate the pavement dynamic re-

*Corresponding author, E-mail address: cauczxm@126.com.

How to cite this article: LIU Xiaolan, ZHANG Xianmin. Finite element modeling and parametric analysis of pavement dynamic responses under moving vehicle load[J]. Transactions of Nanjing University of Aeronautics and Astronautics, 2020, 37(3): 490-500.

http://dx.doi.org/10.16356/j.1005-1120.2020.03.015

sponse based on the moving transient load. Arraigada et al.[9] presented the asphalt pavement response under moving constant load and compared the results with those of accelerated pavement testing. Chun et al.[10] studied the longitudinal strain response at the bottom of asphalt layer under moving constant load. Ramos-García et al.[11] researched the displacement response of the asphalt pavement with modelling the vehicular loading as moving constant load. Li et al.[12] developed the finite element models to simulate pavement responses under falling weight deflectometer (FWD) loading and moving vehicle loading. They explored the influence of vehicle speed and pavement depth on pulse durations of compressive stresses for two asphalt pavement structures. Taherkhani et al. analyzed the effect of tire configuration on the responses of the geogrid-rein forced asphalt pavements under moving transient load[13].

Although previous research has achieved significant advances, the frequency response of pavement structure has not been thoroughly investigated and quantified. Therefore, to better understand the pavement structure dynamic response and performance under moving vehicle load, all pavement indicators, displacement, frequency and strain, need to be investigated and quantified using the finite element (FE) models. The objectives of this study have two folds. The first is to develop and verify the FE model that can accurately reflect pavement displacements, frequencies, and strains. The second is to analyze the important factors that should be considered in the FE models, including asphalt concrete (AC) layer modulus and thickness, base layer modulus and thickness, and subgrade modulus. The development of FE models can directly benefit the AC pavement structure strength evaluation and performance prediction.

1 Finite Element Modeling

1.1 Vehicle model

For the results to be more truly representative of actual pavement vibrations, ANSYS 10.0 simulation software was used to create vehicle-road models in which the mass of the suspension system was assigned to the front and the rear axles of the vehicle in a mass ratio of 1∶4. The testing vehicle was modeled as a three-dimensional mass-spring-damper system with seven degrees of freedom (DOFs), as shown in Table 1 and Fig. 1. The tandems at the drive and the rear axles of the test vehicle were lumped as single wheels for simplicity. Therefore, this model consisted of five rigid masses that represented the truck and its four wheels. The vehicle was assigned three DOFs corresponding to the vertical displacement at the mass center, pitching rotation, and rolling rotation. Each wheel was modeled as a lumped mass with only vertical displacement. The vehicle was represented by beam elements (MPC184). The suspension and non-suspension systems and the moments of inertia of the pitching and rolling rotations were represented by mass elements (Mass21). The spring and damper were represented by a spring-damper element (Combine14).

By using D'Alembert's principle, the equations of motion for the vehicle are

$$m_{cz}\ddot{Z}_0 + K_{xHZ}(Q_1+Q_2)+C_{xHZ}(\dot{Q}_1+\dot{Q}_2)+K_{xQZ}(Q_3+Q_4)+C_{xQZ}(\dot{Q}_3+\dot{Q}_4)=0 \quad (1)$$

$$J_x\ddot{\theta}_x + L_y[K_{xHZ}(Q_1-Q_2)+C_{xHZ}(\dot{Q}_1-\dot{Q}_2)+K_{xQZ}(Q_3-Q_4)+C_{xQZ}(\dot{Q}_3-\dot{Q}_4)]=0 \quad (2)$$

$$J_y\ddot{\theta}_y + L_{HZ}[K_{xHZ}(Q_1+Q_2)+C_{xHZ}(\dot{Q}_1+\dot{Q}_2)]-L_{QZ}[K_{xQZ}(Q_3+Q_4)+C_{xQZ}(\dot{Q}_3+\dot{Q}_4)]=0 \quad (3)$$

$$m_{HZ}\ddot{Z}_5 - K_{xHZ}Q_1 - C_{xHZ}\dot{Q}_1 + K_{LHZ}(Z_5-Z_9)+C_{LHZ}(\dot{Z}_5-\dot{Z}_9)=0 \quad (4)$$

Table 1 Parameters of the test vehicle

Measurement	Parameter
Overall mass / kg	$M_0=3\times10^4$
Mass of suspension system / kg	$m_{cz}=2.7\times10^4$
Mass of front axle / kg	$m_{QZ}=600$
Mass of rear axle / kg	$m_{HZ}=2.4\times10^3$
Mass moment of inertia / (kg•m^2)	$J_x=1.0\times10^6$, $J_y=3.6\times10^5$
Suspension stiffness / (N•m^{-1})	$K_{xQZ}=0.8\times10^6$, $K_{xHZ}=2.0\times10^6$
Tire stiffness / (N•m^{-1})	$K_{LQZ}=1.2\times10^6$, $K_{LHZ}=4.8\times10^6$
Suspension damping / (N•s•m^{-1})	$C_{xQZ}=5.0\times10^3$, $C_{xHZ}=2.0\times10^4$
Tire damping / (N•s•m^{-1})	$C_{LQZ}=6.0\times10^3$, $C_{LHZ}=2.4\times10^4$
Dimension to determine mass center / m	$L_{HZ}=0.9$, $L_{QZ}=3.6$, $L_y=0.9$

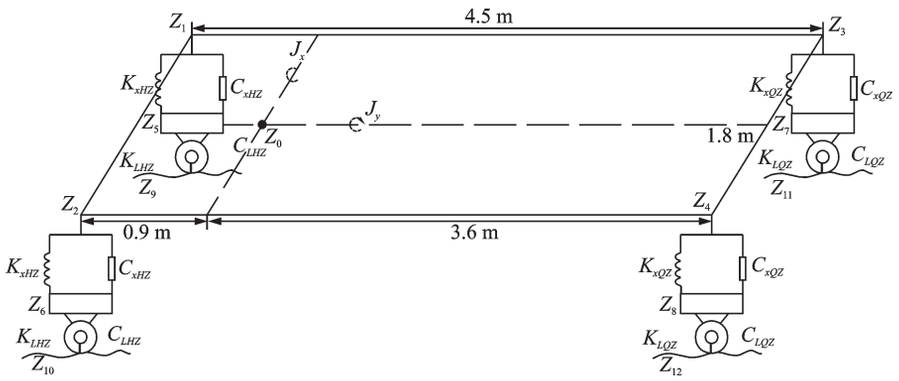

Fig.1 Analytical model of the test vehicle with seven DOFs

$$m_{HZ}\ddot{Z}_6 - K_{xHZ}Q_2 - C_{xHZ}\dot{Q}_2 + K_{LHZ}(Z_6 - Z_{10}) + C_{LHZ}(\dot{Z}_6 - \dot{Z}_{10}) = 0 \quad (5)$$

$$m_{QZ}\ddot{Z}_7 - K_{xQZ}Q_3 - C_{xQZ}\dot{Q}_3 + K_{LQZ}(Z_7 - Z_{11}) + C_{LQZ}(\dot{Z}_7 - \dot{Z}_{11}) = 0 \quad (6)$$

$$m_{QZ}\ddot{Z}_8 - K_{xQZ}Q_4 - C_{xQZ}\dot{Q}_4 + K_{LQZ}(Z_8 - Z_{12}) + C_{LQZ}(\dot{Z}_8 - \dot{Z}_{12}) = 0 \quad (7)$$

where Z_0, Z_1, Z_2, Z_3, Z_4, Z_5, Z_6, Z_7, and Z_8 are the vertical displacements of the salient points of the test vehicle. Furthermore, $Z_1 = Z_0 + \theta_x L_y + \theta_y L_{HZ}$, $Z_2 = Z_0 - \theta_x L_y + \theta_y L_{HZ}$, $Z_3 = Z_0 + \theta_x L_y - \theta_y L_{HZ}$, $Z_4 = Z_0 - \theta_x L_y - \theta_y L_{HZ}$, $Q_1 = Z_1 - Z_5$, $Q_2 = Z_2 - Z_6$, $Q_3 = Z_3 - Z_7$, $Q_4 = Z_4 - Z_8$, where θ_x and θ_y represent the pitching rotation; and Z_9, Z_{10}, Z_{11}, and Z_{12} the road roughness at each of the four wheels, respectively.

1.2 Pavement structure model

The actual pavement structure is a layered architecture, and each structure layer has its own resilient modulus and Poisson's ratio. The pavement structure model of elastic layered system can reflect the actual response of pavement structure. Because pavement structure layers are very complicated, some reasonable assumptions should be made in pavement structure model:

(1) Pavement structure layers are continuous, and the material of each layer is homogeneous and isotropic.

(2) The stress and displacement are continuous in each structure layer.

(3) The stress and displacement in horizontal direction is zero in the infinity point for each pavement structure layer. The stress and displacement in depth direction is zero in the infinity point for subgrade.

However, the infinite entity structure of pavement model is not established by FE method. The finite dimension of pavement model was selected to be 23 m×16 m (length × width) and the depth of subgrade was to be 9 m by calculation and analysis, because the large enough model can reduce the influence of boundary conditions. In the FE model, the eight-node, hexahedral elements with improved calculation accuracy and efficiency (soild45) were used for the mesh generation of pavement structure. The size of mesh element was 23 m×16 mm (length × width) for the asphalt concrete layers and 46 m×32 mm (length × width) for the base layer and subgrade. The mash element thicknesses were selected at 10% of the thickness of the asphalt and the base layers, and 30 mm for the subgrade. The bottom of the subgrade was restricted by all degrees of freedom. The edges of the subgrade and the base layer were constrained in the length-direction and the width-direction. The asphalt concrete layer was stabilized by the interaction with the base layer and the weight of asphalt concrete layer. Table 2[14-16] pres-

Table 2 Properties of the base layer and the subgrade

Layer	Thickness / m	Modulus / MPa	Poisson's ratio	Unit weight / (kg•m^{-3})	Damping ratio / %
Asphalt	0.15—0.35	2 000—6 000	0.25	2 400	5
Base	0.20—0.40	200—34 000	0.35	2 200	5
Subgrade	9	60—220	0.40	1 850	5

ents the properties of the pavement structure layers used in the finite element model.

1.3 Vehicle-pavement model validation

A validation study for the developed FE model was conducted with field measurement results under the traffic speed deflectometer (TSD) and the rolling wheel deflectometer (RWD) testing. The AC pavement section selected for this study was the mainline and closed-loop low-volume road (LVR) of the MnROAD in Wright County, USA. The material properties of pavement structures were obtained from the laboratory testing, TSD and RWD testing, as shown in Table 3[17]. The dynamic load of rear axle at the speed of 13.14 m/s for TSD testing is shown in Fig. 2[17]. And the wheel-pavement contact area of rear axle was 0.0736 m^2. The static and the dynamic contact pressures of RWD testing are 689.5 kPa and 917.04 kPa, respectively[17].

Table 3 Pavement structure layer properties used in the finite element method[17]

Cell	Layer	Thickness / m	Modulus / MPa	Poisson's ratio	Unit weight / (kg•m^{-3})	Damping ratio / %
3	AC	0.076 2	3 817.06	0.25	2 400	5
	Base	1.092 2	472.654	0.35	1 680	5
	Subgrade	3.109 0	121.953	0.4	1 680	5
19	AC	0.127 0	2 073.89	0.25	2 400	5
	Base	0.787 4	220.484	0.35	1 680	5
	Subgrade	4.597 4	42.029	0.4	1 680	5
34	AC	0.101 6	2 060.11	0.25	2 400	5
	Base	0.304 8	108.173	0.35	1 760	5
	Subgrade	1.176 0	58.565	0.4	1 760	5

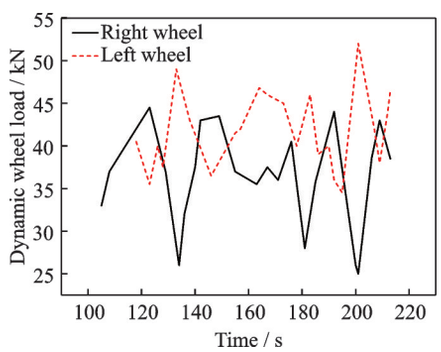

Fig.2 Dynamic wheel load for TSD testing[17]

The above data were directly input into the ANSYS 10.0 simulation software to establish the FE model of wheel-pavement response. In the FE model, the AC pavement structures were simulated as the elastic layered system. The finite dimension of pavement model was selected to be 23 m×16 m (length × width) and the depth of pavement structure was as shown in Table 3. The eight-node, and the hexahedral elements with improved calculation accuracy and efficiency (soild45) were used for the mesh generation of pavement structure. The size of mesh element was 23 m×16 mm (length × width) for the AC layers and 46 m×32 mm (length × width) for the base layer and the subgrade. The mash element thicknesses were selected at 10% of the thickness of the AC layers, the base layers and the subgrade. The bottom of the subgrade was restricted by all degrees of freedom. The edges of the subgrade and the base layer were constrained in the length-direction and the width-direction. The AC layer was stabilized by the interaction with the base layer and the weight of the AC layer. The vehicle load was simplified by using the measured dynamic loading amplitude in Fig.2 within the tire imprint area of 0.073 6 m^2 in the TSD testing. The vehicle load was simplified by using contact pressures in the RWD testing. To simulate the movement of a wheel at a certain speed, the concept of a continuously moving load was used. In this approach, the wheel loading imprint area is gradually shifted over the pavement. The step time was decided by the wheel moving speed and element lengths.

These data were directly used in the FE model as the input and the accuracy of prediction results was and compared to field measurements examined for model validation. Fig. 3 compares the measured and the predicted surface displacement. The results

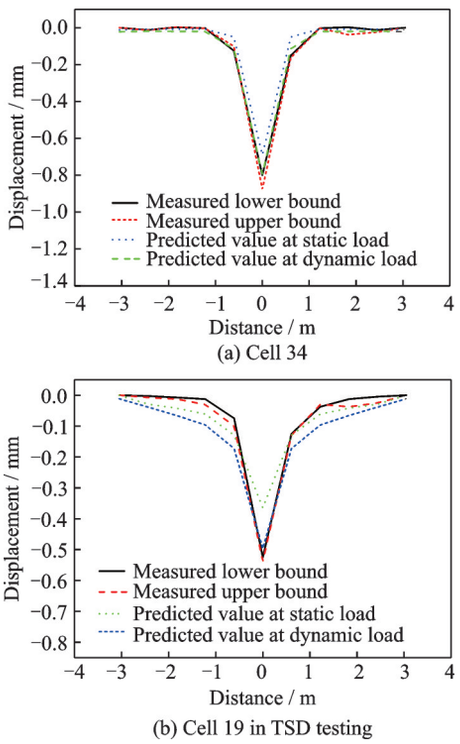

(a) Cell 34

(b) Cell 19 in TSD testing

Fig.3 Predicted and measured surface displacements in TSD testing

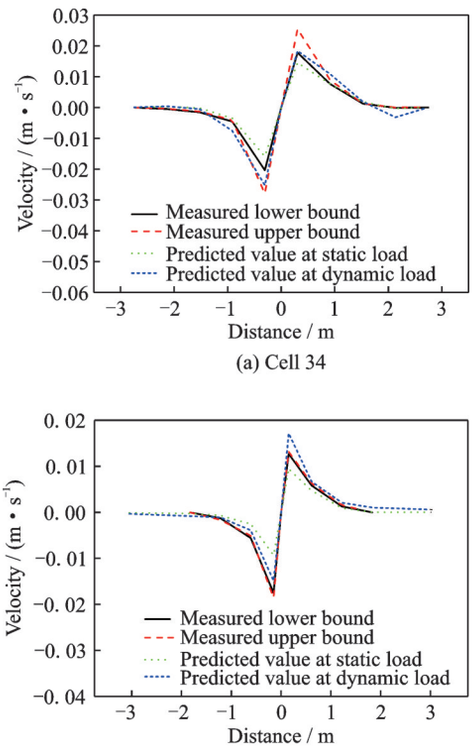

(a) Cell 34

(b) Cell 19

Fig.4 Predicted and measured surface velocities in TSD testing

show that the FE model of cell 34 adequately captured the shape of measured displacements, while the finite element model displacement basins were wider than the measured values of cell 19. It might be caused by the transverse wheel wander. The FE model results of dynamic load had good agreements with the maximum displacement. Fig.4 compares the predicted and the measured surface velocities (maximum from field trials). Although all finite element model case results had similar shapes as the measured ones, the predictions of dynamic load were closer to the measured velocities. Fig.5 compares the measured and the predicted longitudinal strains. The calculated longitudinal strains from the finite element model of dynamic load matched well with the measured values. In a word, the realistic assumption of vehicle-pavement interaction and dynamic load pattern resulted in smaller differences between the measured and the calculated displacements, the velocities and the longitudinal strains. Hence, the vehicle-pavement model can predict the pavement response with dynamic vehicle load moving on different asphalt pavements.

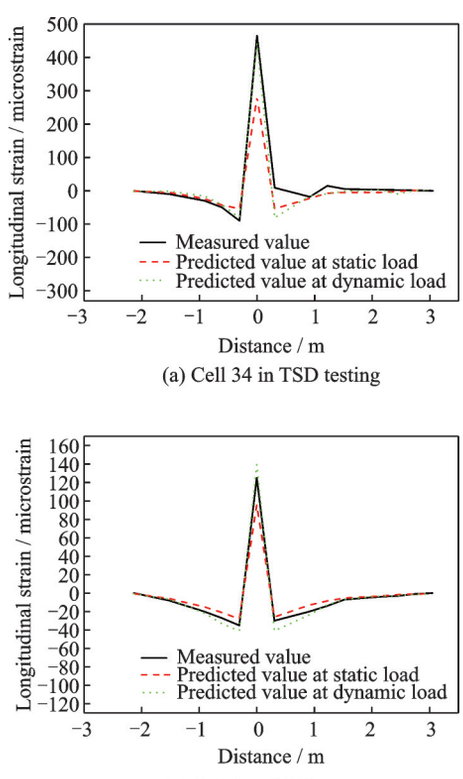

(a) Cell 34 in TSD testing

(b) Cell 3 in RWD testing

Fig.5 Predicted and measured longitudinal strains for cell 34 in TSD testing and for cell 3 in RWD testing

2 Results and Analysis

The influence of pavement structure modulus and thickness on pavement responses, including surface displacement, frequency and strain, under vehicle dynamic loading were investigated using the developed FE model. The surface displacement can represent structure behavior of the entire pavement system[12]. It has been widely accepted that tensile strains at the bottom of asphalt concrete layer are related to fatigue cracking distress and tensile strains at the top of subgrade are related to rutting. In addition, the frequency was used to indicate the vibration performance of vehicle and pavement interaction, because the frequency can better represent the integrity of the pavement system than surface displacement and strain do.

2.1 Surface displacement analysis

Fig.6 shows the influences of the asphalt concrete layer modulus and thickness, the base layer modulus and thickness, and the subgrade modulus on surface displacements. When the parameter of pavement structure keeps the same, both the displacement basin width and the maximum value of dynamic surface displacements are larger than those of static surface displacements.

In Figs.6(a) and (b), the shape of surface displacement is similar and the maximum of surface displacement is various at different asphalt concrete layer moduli and thicknesses. When the asphalt concrete layer modulus increases from 2 000 MPa to 4 000 MPa, the maximum of dynamic surface displacement decreases 0.11 mm. And as the asphalt concrete layer modulus increases from 4 000 MPa to 6 000 MPa, the maximum of dynamic surface displacement decreases 0.06 mm. However, the maximum of dynamic surface displacement decreases 0.10 mm with the asphalt concrete layer thickness increasing from 0.15 m to 0.35 m. Since the addition of asphalt concrete layer modulus and thickness is beneficial to improving the strength of the entire pavement system and reducing the surface displacement. Furthermore, the asphalt concrete layer modulus of more than 4 000 MPa has little effect on the surface displacement. Therefore, the blindly increasing of asphalt concrete layer modulus might have minimal effectiveness on the reduction of surface displacement and the improvement of pavement structure performance.

In Figs.6(c) and (d), the maximum value and decreasing amplitude of surface displacement decreases with the increase of base layer moduli and thicknesses. When the base layer modulus increases from 200 MPa to 1 800 MPa, the maximum of dynamic surface displacement decreases 0.04 mm uniformly, and the dynamic surface displacement in the middle of two wheels decreases 0.07 mm. As the base layer modulus increases from 1 800 MPa to 3 400 MPa, the maximum of dynamic surface displacement decreases 0.034 mm uniformly, and the dynamic surface displacement in the middle of two wheels decreases 0.035 mm. Hence, the surface displacement in the middle of two wheels is close to the maximum of surface displacement as the increase of the base layer moduli. Especially, the surface displacement in the middle of two wheels is similar to the maximum of surface displacement with the base layer modulus more than 1 800 MPa. Meanwhile, surface displacement decreases with the increase of the base layer thickness. When the base layer thickness is more than 0.30 m, the increasing amplitude of surface displacement is smaller. Hence, the base layer modulus of 1 800 MPa and the base layer thickness of 0.30 m can help to ensure quality and save cost for the pavement engineering.

In Fig.6(e), both the shape and the maximum of surface displacement vary with different subgrade moduli. The maximum of the dynamic surface displacement reduces 0.26 mm with the subgrade modulus from 60 MPa to 180 MPa, and decreases

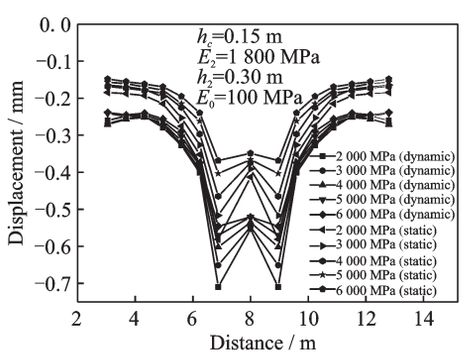

(a) Surface displacement influenced by the asphalt concrete layer modulus

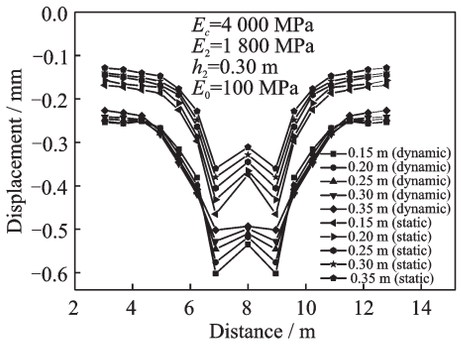

(b) Surface displacement influenced by asphalt concrete layer thickness

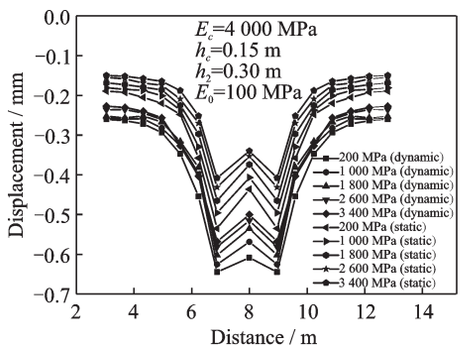

(c) Surface displacement influenced by base layer modulus

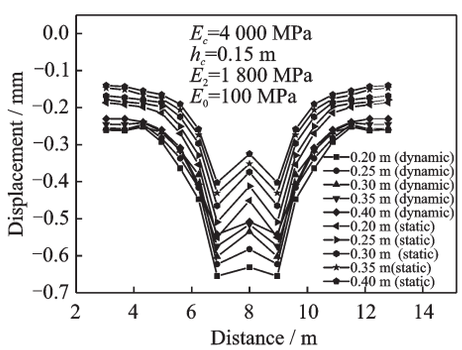

(d) Surface displacement influenced by base layer thickness

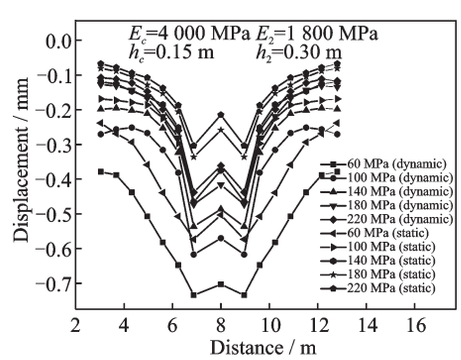

(e) Surface displacement influenced by subgrade modulus

E_c—Asphalt concrete layer modulus

h_c—Asphalt concrete layer thickness

E_2—Base layer modulus

h_2—Base layer thickness

E_0—Subgrade modulus

Fig.6 Surface displacement influenced by different factors

0.03 mm as the subgrade modulus increasing from 180 MPa to 220 MPa. Nevertheless, when the subgrade modulus varies from 60 MPa to 180 MPa, the dynamic surface displacement in the middle of two wheels decreases 0.29 mm. As the subgrade modulus varies from 180 MPa to 220 MPa, the dynamic surface displacement at the middle of two wheels decreases 0.05 mm. Thereby, the subgrade moduli have a significant influence on the maximum of surface displacement and the surface displacement in the middle of two wheels when the subgrade modulus is less than 180 MPa. In other words, it is inadvisable to reduce surface displacements and promote the pavement performance by blindly increasing subgrade modulus.

In a nutshell, these findings indicate that the influence of subgrade modulus on surface displacement is more remarkable than those of asphalt concrete layer modulus and thickness, and base layer modulus and thickness. In addition, asphalt concrete layer modulus, base layer modulus and thickness, and subgrade modulus have an optimal value.

2.2 Frequency analysis

Fig.7 shows the acceleration-time histories and frequency spectrum analysis of acceleration. The acceleration-time histories of pavement free vibration were obtained by taking impulsive load as excitation

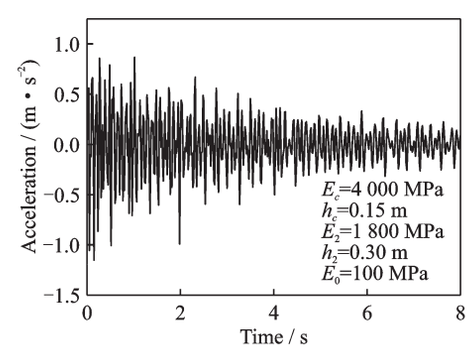

(a) Acceleration-time histories

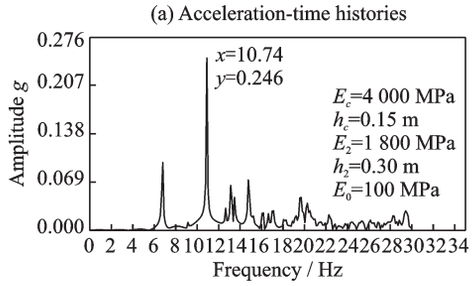

(b) Frequency spectrum analysis of acceleration

Fig.7 Acceleration

source and the central point of pavement as sampling position. The method of fast Fourier transform was applied to obtain the frequency spectrum analysis of acceleration. The sampling frequency must be more than twice of the original signal frequency to reflect the actual frequency domain signals, which is required in sampling theorem. Moreover, the frequency range of pavement vibration was mainly 0 Hz to 30 Hz. Therefore, the sampling in this study was selected as 60 Hz. In other words, 300 acceleration signals were collected in 5 s.

Fig.8 shows the influence of the asphalt concrete layer modulus and thickness, the base layer modulus and the thickness, and subgrade modulus on the frequency of pavement structure. Figs.8(a), (b) indicate that the frequency increases 0.24 Hz as the asphalt concrete layer modulus increasing from 2 000 MPa to 6 000 MPa, and 0.48 Hz as the asphalt concrete layer thickness increasing from 0.35 m to 0.15 m. Thereby, the frequency is positively correlated with asphalt concrete layer moduli, and negatively correlated with asphalt concrete layer thicknesses. Moreover, the increasing of asphalt concrete layer thickness causes the decreasing of the pavement frequency, which is easy to make the frequency of pavement structure being close to that of vehicle load and contribute to the resonance of pavement structure and vehicle load. It is not feasible for improving the strength of pavement structure by blindly increasing the asphalt concrete layer thickness.

Figs.8(c) and (d) show that influences of base layer moduli are the same as those of asphalt concrete layer moduli, and effects of base layer thicknesses are similar to those of asphalt concrete layer thicknesses. The frequency of pavement structure increases with the addition of the base layer modulus and the reduction of the base layer thickness. The influence of the asphalt concrete layer modulus on the frequency is greater than that of the base layer modulus.

Fig.8(e) indicates that the effect of subgrade moduli on frequency is more significant than those of asphalt concrete layer moduli and thickness, and base layer moduli and thickness. The increase of the subgrade modulus is helpful to improve the frequency of pavement structures. Furthermore, when the subgrade modulus varies from 60 MPa to 220 MPa, the frequency increases about 0.97 Hz. It means that the subgrade modulus is the critical factor for pavement structure performance. Attentions should be paid to subgrade moduli in the design and maintenance of pavement structure.

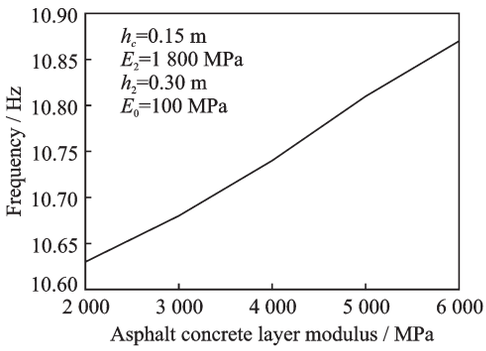

(a) Frequency influenced by asphalt concrete layer modulus

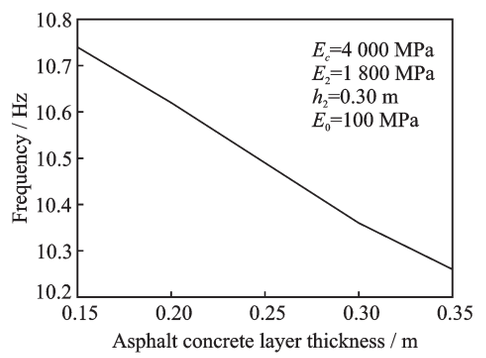

(b) Frequency influenced by asphalt concrete layer thickness

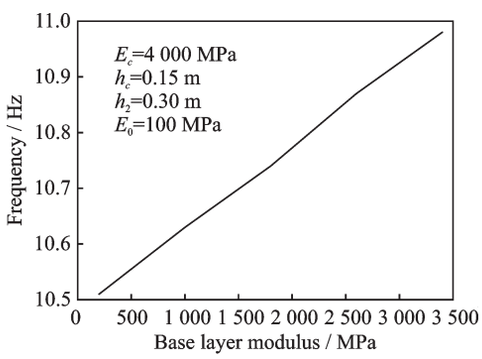

(c) Frequency influenced by base layer modulus

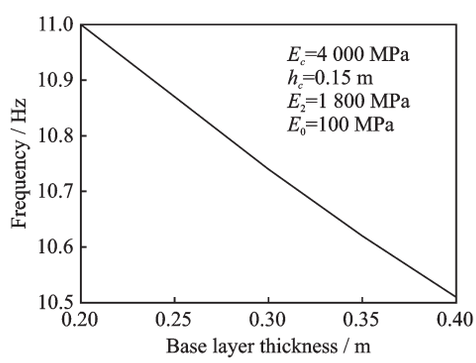

(d) Frequency influenced by base layer thickness

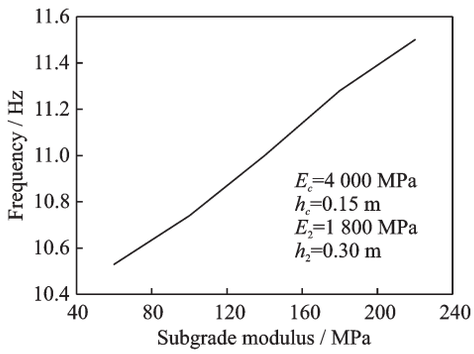

(e) Frequency influenced by subgrade modulus

Fig.8 Frequency influenced by different factors

The recent advances in optoelectronic oscillators, arbitrary waveform generation, photonic mixing, phase coding, filtering, beamforming, analog-to-digital conversion, and stable RF signal transfer are described. Challenges in implementation of these components and subsystems for meeting the requirements of the radar applications are discussed.

2.3 Strain analysis

Fig.9 shows the influence of the asphalt concrete layer modulus and thickness, the base layer modulus and thickness, and the subgrade modulus on tensile strains. When the parameter of pavement structure keeps the same, the dynamic tensile strain is larger than the static tensile strain. The shapes of the tensile strain in Fig.9 are similar and the maximum value of tensile strain is at the bottom of asphalt concrete layer for different pavement structures. The reason is that the tensile strain decreases with the increase of pavement structure depth, and the surface of asphalt concrete layer is mainly compressive strain. Therefore, tensile strains at bottom of the asphalt concrete layer are important to evaluate the bottom-up cracking distress. In Figs.9(a), (c), both the asphalt concrete layer and the base layer moduli have a negative relationship with tensile strains. The maximum of dynamic tensile strain decreases about 74 με as the asphalt concrete layer modulus increasing from 2 000 MPa to 6 000 MPa, and 80 με as the base layer modulus increasing from 200 MPa to 3 400 MPa.

Since the main focus is the comparison of tensile strain (shape and maximum value), the plots are shifted to align so that the maximum tensile strain locations can coincide. In Figs.9(b) and (d), when the asphalt concrete layer thickness increases from 0.15 m to 0.30 m, the maximum of dynamic tensile strain decreases 51 με. As the base layer thickness increases from 0.20 m to 0.35 m, the maximum of dynamic tensile strain decreases 38 με. However, the maximum of dynamic tensile strain decreases 11 με with the asphalt concrete layer thickness rising from 0.30 m to 0.35 m, and 10 με as the base layer thickness growing from 0.35 m to 0.40 m. Therefore, the influence of the asphalt concrete layer thickness on tensile strain is greater than that of base layer thickness.

In Fig.9(e), the shape and maximum of tensile strains vary largely when the subgrade modulus is more than 60 MPa. For example, the maximum of dynamic tensile strain decreases about 19 με as the subgrade modulus rising from 60 MPa to 100 MPa, and the maximum of dynamic tensile strain decreases 33 με as the subgrade modulus rising from 100 MPa to 220 MPa. Thereby, the influence of subgrade moduli on the tensile strain is not negligible.

In conclusion, the surface displacement, frequency and strain of pavement structure are all effected by parameters of pavement structures. Subgrade moduli have a significant influence and could not be

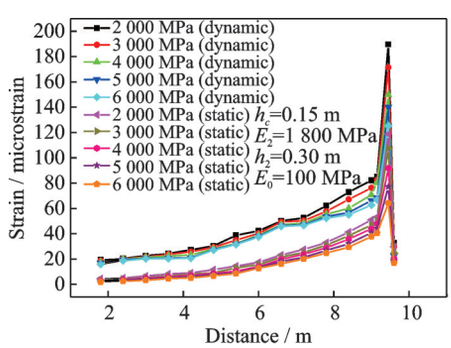

(a) Strain influenced by asphalt concrete layer modulus

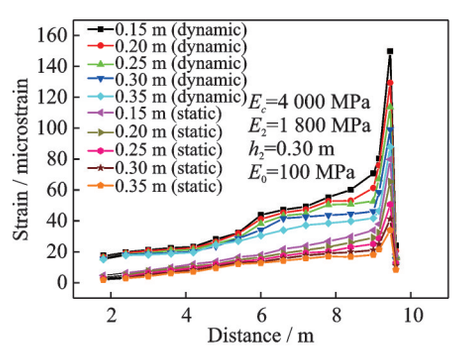

(b) Strain influenced by asphalt concrete layer

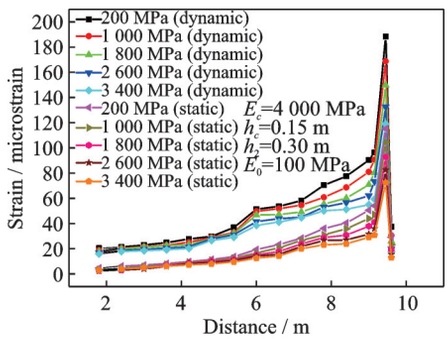

(c) Strain influenced by base layer modulus

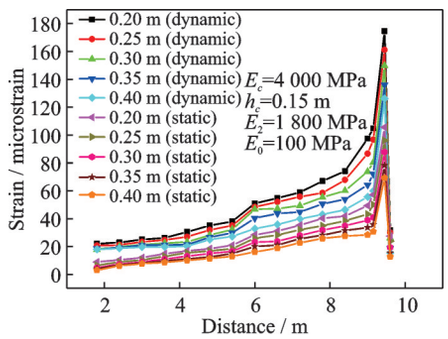

(d) Strain influenced by base layer thickness

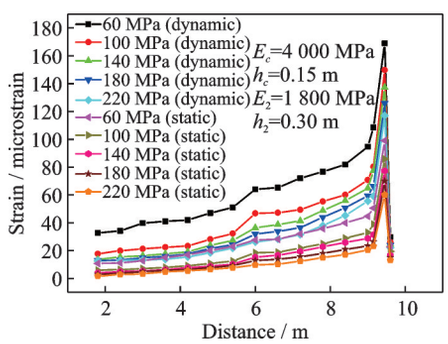

(e) Strain influenced by subgrade modulus

Fig.9 Strain influenced by different factors

disregarded. Fig.9 also shows that tensile strains have a turning point at the distance of 6 m (3 m away from the top of the subgrade). The tensile strain at the distance of 6 m to 9 m varies larger and changes faster than that at the distance of 1.3 m to 6 m. Parameters of pavement structures have little influence on tensile strain at the distance of 1.3 m to 6 m.

3 Conclusions

In this study, FE models were developed to simulate asphalt pavement dynamic response under moving vehicle loading. The parametric analysis findings demonstrate subgrade moduli are the important factor for the surface displacement, frequency and strain. Asphalt concrete layer moduli have small influence on the surface displacement, frequency and strain. When the parameter of pavement structure keeps the same, both the displacement basin width and the maximum value of dynamic surface displacements are larger than those of static surface displacements. The frequency response of the entire pavement structure is larger than the response of the surface displacement and strain, especially the effect of subgrade moduli. The frequency increases with the addition of pavement structure layer modulus and the reduction of pavement structure layer thickness. The shapes of the dynamic and the static tensile strains are similar. With the same parameters of a pavement structure, the maximum value of the dynamic tensile strain is larger than that of the static tensile strain. The developed FE model successfully captures the surface displacement, frequency, and strain of asphalt concrete pavement.

References

[1] GARCIA G, THOMPSON M R. Strain and pulse duration considerations for extended-life hot-mix asphalt pavement design[J]. Transportation Research Record Journal of the Transportation Research Board, 2008, 2087: 3-11.

[2] PICOUX B, AYADI E L, PETIT C. Dynamic response of a flexible pavement submitted by impulsive loading[J]. Soil Dynamics and Earthquake Engineering, 2009, 29(5): 845-854.

[3] WANG H, AL-QADI I L. Impact quantification of wide-base tire loading on secondary road flexible pavements[J]. Journal of Transportation Engineering, 2011, 137(9): 630-639.

[4] OZER H, AL-QADI I L, WANG H, et al. Characterisation of interface bonding between hot-mix asphalt overlay and concrete pavements: Modelling and in-situ response to accelerated loading[J]. International Journal of Pavement Engineering, 2012, 13(2): 181-196.

[5] WANG H, AL-QADI I L. Importance of nonlinear anisotropic modeling of granular base for predicting maximum viscoelastic pavement responses under moving vehicular loading[J]. Journal of Engineering Mechanics, 2013, 139(1): 29-38.

[6] AL-QADI I L, WANG H, TUTUMLUER E. Dynamic analysis of thin asphalt pavements by using cross-anisotropic stress-dependent properties for granular layer[J]. Transportation Research Record Journal of the Transportation Research Board, 2015, 2154: 156-163.

[7] PATIL V A, SAWANT V A, DEB K. 3D finite-ele-

ment dynamic analysis of rigid pavement using infinite elements[J]. International Journal of Geomechanics, 2013, 13(5): 533-544.
[8] DONG Z H, NI F Y. Dynamic model and criteria indices of semi-rigid base asphalt pavement[J]. International Journal of Pavement Engineering, 2014, 15(9): 854-866.
[9] ARRAIGADA M, ANDRES P, PARTL M N, et al. Effect of full-size and down-scaled accelerated traffic loading on pavement behavior[J]. Materials and Structures, 2014, 47(8): 1409-1424.
[10] CHUN S, KIM K, GREENE J, et al. Evaluation of interlayer bonding condition on structural response characteristics of asphalt pavement using finite element analysis and full-scale field tests[J]. Construction and Building Materials, 2015, 96: 307-318.
[11] RAMOS-GARCÍA J A, CASTRO M. Linear viscoelastic behavior of asphalt pavements: 3D-FE response models[J]. Construction and Building Materials, 2017, 136: 414-425.
[12] LI M, WANG H, XU G, et al. Finite element modeling and parametric analysis of viscoelastic and nonlinear pavement responses under dynamic FWD loading[J]. Construction and Building Materials, 2017, 141: 23-35.
[13] TAHERKHANI H, JALALI M. Viscoelastic analysis of geogrid-reinforced asphaltic pavement under different tire configurations[J]. International Journal of Geomechanics, 2018, 18(7): 04018060.
[14] CCCC Highway Consultants. Specifications of cement concrete pavement design for highway: JTG D40—2002[S]. Beijing, China: China Communications Press, 2006.(in Chinese)
[15] ZHANG Xianmin, CHEN Xinchun, DONG Qian, et al. PCN calculation method for composite pavement based on equivalent displacement[J]. Journal of Nanjing University of Aeronautics and Astronautics, 2015, 47(4): 532-538.(in Chinese)
[16] HEIMBS S, CICHOSZ J, KLAUS M, et al. Sandwich structures with textile-reinforced composite foldcores under impact loads[J]. Composite Structures, 2010, 92(6): 1485-1497.
[17] GONZALO R, RAD A, SOHEIL N, et al. Strain and pulse duration considerations for extended-life hotmix asphalt pavement design[J]. Transportation Research Record Journal of the Transportation Research Board, 2016, 2087: 3-11.

Acknowledgement This paper was supported by the National Natural Science Foundation of China (No.51178456).

Authors Dr. **LIU Xiaolan** received B.S. degree in Highway and Railway Engineering from Civil Aviation University of China (CAUC) in 2016 and Ph.D. degree in Highway and Railway Engineering from Nanjing University of Aeronautics and Astronautics (NUAA) in 2019, respectively. Her research is focused on pavement structure responses and bearing capacity evaluation.

Prof. **ZHANG Xianmin** received the B.S. and Ph.D. degrees in geotechnical engineering from Tianjin University, Tianjin, China, in 1990 and 1995, respectively. From 2000 to present, he is the director in Airport College of CAUC. From 2008 to present, he is doctoral tutor at the College of Civil Aviation, NUAA. His research has focused on pavement structure responses and nondestructive testing.

Author contributions Dr. **LIU Xiaolan** designed the study, complied the models, conducted the analysis, interpreted the results and wrote the manuscript. Prof. **ZHANG Xianmin** contributed to the discussion and background of the study. All authors commented on the manuscript and approved the submission.

Competing interests The authors declare no competing interests.

(Production Editor: ZHANG Bei)

移动车辆荷载作用下道面动态响应的有限元模型和参数分析

刘小兰[1], 张献民[2,3]

(1.天津城建大学土木工程学院,天津 300384, 中国; 2.南京航空航天大学民航学院, 南京 211106, 中国; 3.中国民航大学机场学院, 天津 300300, 中国)

摘要:为建立能够模拟车辆动荷载作用于道面的有限元模型,进而较为真实的反映车辆和道面的相互作用时道面的响应,分析了沥青面层模量和厚度、基层模量和厚度,以及路基模量对路表弯沉、频率和应变的影响规律。分析结果表明:动态路表弯沉的弯沉盆宽度和最大值均大于静态路表弯沉;频率与道面结构模量正相关,与道面结构厚度负相关;道面结构不同深度处动态和静态拉应变的形状相似;动态拉应变的最大值大于静态拉应变。整个道面结构的频率响应比路表弯沉和应变响应更显著。路基模量对路表弯沉、频率和应变具有显著影响。

关键词:道面动态响应;车辆荷载;路表弯沉;频率;应变